Effect of Si/Al Ratio on SSZ-13 Crystallization and Its Methanol-To-Olefins Catalytic Properties

Zhiqiang Xu, Hongfang Ma, Haitao Zhang, Weixin Qian, Weiyong Ying

Abstract—SSZ-13 materials with different Si/Al ratio were prepared by varying the composition of aluminosilicate precursor solutions upon hydrothermal treatment at 150 °C. The Si/Al ratio of the initial system was systematically changed from 12.5 to infinity in order to study the limits of Al composition in precursor solutions for constructing CHA structure. The intermediates and final products were investigated by complementary techniques such as XRD, HRTEM, FESEM, and chemical analysis. NH_3-TPD was used to study the Brønsted acidity of SSZ-13 samples with different Si/Al ratios. The effect of the Si/Al ratio on the precursor species, ultimate crystal size, morphology and yield was investigated. The results revealed that Al species determine the nucleation rate and the number of nuclei, which is tied to the morphology and yield of SSZ-13. The size of SSZ-13 increased and the yield decreased as the Si/Al ratio was improved. Varying Si/Al ratio of the initial system is a facile, commercially viable method of tailoring SSZ-13 crystal size and morphology. Furthermore, SSZ-13 materials with different Si/Al ratio were tested as catalysts for the methanol to olefins (MTO) reaction at 350 °C. SSZ-13 with the Si/Al ratio of 35 shows the best MTO catalytic performance.

Keywords—Crystallization, MTO, Si/Al ratio, SSZ-13.

I. INTRODUCTION

METHANOL TO OLEFINS (MTO) conversion as a non-oil route to produce light olefins has aroused extensive attention and has been comprehensively studied. Various solid acids were used to catalyze this reaction. HZSM-5, HSAPO-34, and HSSZ-13 show excellent catalytic properties in the MTO reaction [1], [2].

SSZ-13 is zeolite analogue of SAPO-34 with consistent CHA structure, and it shows excellent light olefins selectivity, which can reach over 80% [3], [4]. Compared with SAPO-34, SSZ-13 catalyzes MTO reaction at a lower temperature around 350 °C because of its stronger acid sites [5]. However, the hydrogen transfer reaction is severe at beginning of the MTO reaction, leading to high propane selectivity, and a short lifetime. To improve SSZ-13 MTO catalytic properties, the most direct way is to increase its Si/Al ratio. In SSZ-13, the oxgen bridge between Al^{3+} and Si^{4+} needs a cation to keep electroneutral, and an Brønsted acid site can be created when the cation is exchanged to an hydrogen ion. So, the acid density can be decreased easily by increasing Si/Al ratio of SSZ-13. Moreover, Deimund et al. found that increasing Si/Al ratio could decrease Al-O-Si-O-Al bond, which is known as a

Zhiqiang Xu, Hongfang Ma, Haitao Zhang, Weixin Qian, and Weiyong Ying are with Engineering Research Center of Large Scale Reactor Engineering and Technology, East China University of Science and Technology, Shanghai 200237, China (e-mail: 13162168201@163.com, mark@ecust.edu.cn, zht@ecust.edu.cn, wxqian@ecust.edu.cn, wying@ecust.edu.cn).

paired site. And the propane selevities in the initial period of MTO reaction could be impaired remarkably and lifetime was improved with the decrease of paired Al sites [6]. The common way to vary zeolites Si/Al is changing the relative amounts of Al for zeolites in the respective synthesis gel [7], [8]. Al amount in the initial gel changes zeolites element composition and has an impact on the zeolites particle morphology, crystallinity, and yield. For example, ZSM-5 [9], HBEA [10] synthesized with different Si/Al molar ratios had different morphologies and particle sizes. It was found that the average ZSM-5 crystal size increased as Si/Al molar ratio increased. In MTO reaction, smaller particle size and higher crystallinity can enhance the MTO catalytic properties. Small grain size can reduce diffusion distance and reduce coke deposition speed [11]-[14]. In this paper, we change the Si/Al ratio of aluminosilicate precursor and investigated its effect on SSZ-13 particles nucleation and morphology. Eventually, the MTO properties of all samples were evaluated, and SSZ-13 synthesized from precursor with Si/Al ratio of 35 shows the longest lifetime.

II. EXPERIMENTAL SECTION

A. Catalyst Preparation

The chemicals used in the synthesis were N,N,N-trimethyl - 1-adamantammonium hydroxide (TMAdaOH, 25 wt. %, Nanjing Chemlin Chemical Industrial Co.), fumed silica (0.007 m average particle size, Aldrich), Tetraethylortho-silicate (TEOS, Shanghai Lingfeng Chemical Reagent Co.), aluminium iso-propoxide (Al(OPri)₃, Shanghai Macklin Biochemical Co.), all chemicals were used without further purification.

The gel composition of SSZ-13 was as follows:20 TMAdaOH: $10Na_2O$:xAl_2O_3:$100SiO_2$:$4400H_2O$. (x was varied from 0 to 4). First, NaOH was dissolved in H_2O followed by sequential addition of Al(OPri)₃ and TMAdaOH. The solution was kept under stirring conditions at room temperature until it became clear, followed by the slow addition of fumed silica. The gel was then aged for 24 h before being placed in a Teflon lined autoclave in a rotating oven at 150 °C for 5 days. All materials were calcined at 550 °C for 6h to remove template. The calcined materials were then converted to the ammonium form by ion exchanging for three times with 1 M aqueous NH_4Cl solution at 90 °C for 2 h, and then were washed with water. The solid product was seperated from liquid by centrifugation of 4500 r/min. Then, these samples were dried overnight at 110 °C and calcined at 550 °C for 6h to convert them to the proton form.

The sample is denoted as HS-y, where y represents the

Si/Al ratio in initial gel. Specially, the sample prepared without aluminum source is denoted as HS-∞.

B. Catalytic Performance Test

The MTO reaction was carried out in a fixed bed at 350 °C under atmospheric pressure. 500 mg sample (40-60 mesh) was packed on quartz wool plugging inside the stainless steel reactor (i.d: 0.8 cm, length: 65 cm). Pure methanol was fed into pre-heater kept at 200 °C with a flow rate of 0.01 ml/min by an advection pump (2PB00C, Beijing Satellite Manufacturing Factory, China). Nitrogen used as an inert diluents gas was co-fed with methanol into pre-heater at 60 ml/min. The space velocity in WHSV was kept to 1 h^{-1}. The analysis of the reaction product was performed on online chromatographs: Agilent GC 7890B equipped with TCD, Front FID and Back FID with RT-Q-Bond, DB-WAX, Plot-Q columns. The concentration of methanol in uncooled product effluent was investigated by Back FID. The dimethyl ether and hydrocarbons were detected by Front FID. Dimethyl ether was considered as a reactant in the calculation of the conversion and selectivity.

C. Characterization

The XRD patterns were recorded on a Rigaku D-max 2,200 X-ray diffractometer using Cu-Ka radiations. Nitrogen adsorption–desorption measurements were carried out at -196 °C on Micromeritics ASAP 2020M analyzer, after the samples were degassed at 350 °C for 6h. The specific surface areas were calculated according to the BET method. The micropore volume and surface area were calculated using t-plot method. Crystal morphology, size, and particle size distribution were assessed by field emission scanning electron microscopy (FESEM Nova NanoSEM-450) and transmission electron microscope (TEM JEM-2100). NH_3-TPD was performed on Micromeritics AutoChemII 2920. Typically, 200 mg of samples was pretreated at 550 °C for 2h in He flow (40 ml/min) and subsequently cooled to adsorption temperature of 100 °C. The gas mixture of NH_3:He (10 vol.% of NH_3) was passed through the sample at the rate of 30 mL/min for 30 min. After a 60 min purge in flowing helium (40 mL/min) to remove weakly adsorbed NH_3, the sample was heated to 650 °C at a rate of 10 °C/min in He flow (40 mL/min).

III. RESULTS AND DISCUSSION

XRD of all samples was shown in Fig. 1, all samples except for HS-∞ presented typical CHA diffraction peak. It could be concluded that precursor was unable to crystalize to SSZ-13 without Al source. The relative crystallinity was determined from the main peak intensities at 2θ≈9.6, 13.0, and 20.6 on the base of HS-12.5 possessing the highest XRD intensities among all samples. The relative crystallinity of samples was calculated by the following equation.

$$Relative\ crystallinity = I/I_0$$

where I is the line intensity of the sample, and I_0 is the line intensity of the HS-25. From Table I, the crystalline of SSZ-13

showed an obvious decline at the Si/Al ratios of 12.5 and 80. Excessive low or high Si/Al ratio is not beneficial to the crystallization of SSZ-13. The synthesis yield (Ys) was defined as the g of calcined solid per g of SiO_2 and Al_2O_3 in the initial mixture. The yield of HS-80 is lower than other samples. The direct synthesis of high silica SSZ-13 may face the problem of the low yield.
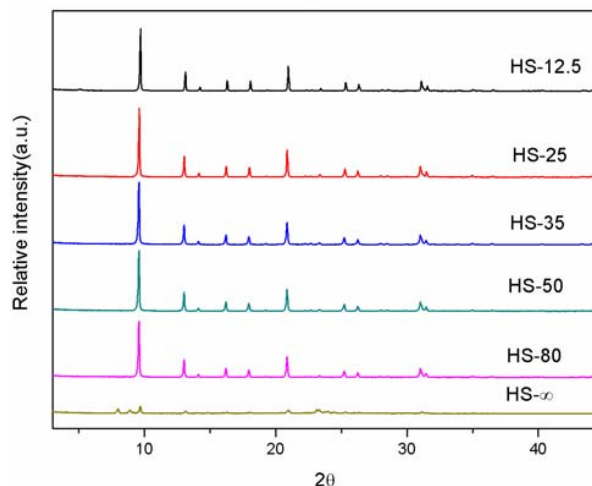

Fig. 1 Powder XRD patterns of the of all samples

The SEM images of samples were shown in Fig. 2. Fig. 2 (A) shows HS-12.5 particles with the average size of 525 nm and ellipsoid shape. The external surface of HS-12.5 is full of small protuberances with size of 5~10 nm. With the improvement of Si/Al ratio, SSZ-13 particles become larger. The average sizes of HS-35 and HS-80 are 775 nm and 3350 nm, respectively. The shape of crystals turned to be cube. The SEM images of precursor after 36h hydrothermal treatment were shown in Fig. 3. We can see that the precursor of SSZ-13 has nucleated, and the size of nucleation is identified with the final grain size. During SSZ-13 crystallization process, the amount of Al source determined nucleation speed and nuclease quantity, which has an impact on SSZ-13 morphology. In low Si/Al ratio condition, the amorphous aluminosilicate particles assemble together and form SSZ-13 crystal grains [15]. Crystallization by particle attachment seemingly plays a dominant role, leading to the formation of spherical, highly roughened crystals. When the Si/Al ratio is improving, SSZ-13 particles tend to grow layer by layer in an classical ways, as a result, sample HS-80 presents a cube-like shape. It seems that varying Si/Al ratio in initial gel can change the crystallization way. The size and morphology of the crystals depend on the Si/Al molar ratio used.

The textural prosperities of SSZ-13 samples were determined using N_2 adsorption-desorption measurements and the results are shown in Table I. All of the samples show type-I N_2 adsorption/desorption isotherms in Fig. 4. The uptake near saturation pressure in the isotherms can be observed in the sample HS-12.5. The phenomenon is most probably related to space filling in grain boundaries or pinholes between

small SSZ-13 crystals. Moreover, samples synthesized from low Si/Al initial gel possess larger external surface area compared with that with high Si/Al ratio. The phenomenon is related to small particle size of low Si/Al ratio sample. The result is in accordance with the XRD patterns and SEM images.
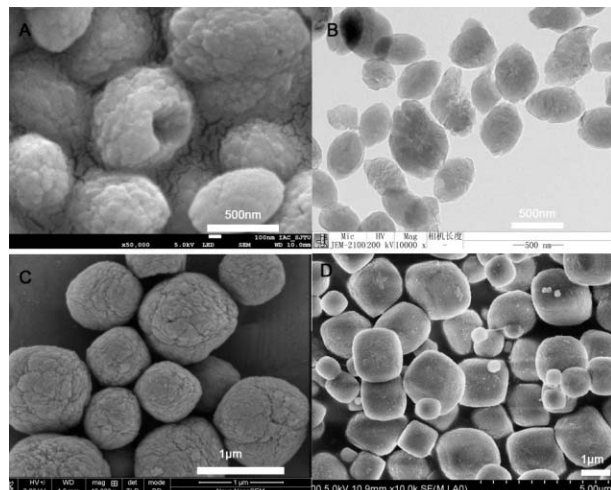

Fig. 2 SEM images of HS-12.5 (A), HS-25 (C), HS-80(D); TEM image of HS-12.5 (B)
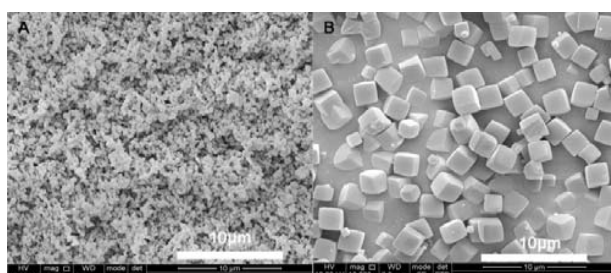

Fig. 3 SEM images of a sample HS-12.5(A) and HS-80(B) after 36 h of heating

TABLE I
TEXTURAL PROPERTIES, RELATIVE CRYSTALLINITY AND YIELD FOR SSZ-13

Sample	BET Surface Area (m²/g)	V_{total} (cm³/g)	$S_{external}$ (cm³/g)	Relative Crystallinity (%)	Yield (%)
HS-12.5	580.4	0.32	45.3	81.6	71.3
HS-25	624.2	0.33	43.1	100	72.4
HS-35	654.4	0.33	34.1	94.1	75
HS-50	629.7	0.34	19.2	90.2	67.3
HS-80	570.1	0.33	20.2	83.6	62.1

The acid sites strength and quantities of all samples were investigated by NH_3-TPD. All samples present two clear peaks at 150-180 and 385-480 °C, which corresponded to weak sites and strong acid sites. The strong acid sites are mostly contributed by the Brønsted acid sites which are formed by the counteractions required to balance the substitution of Al^{3+} for Si^{4+} in the zeolite framework [16]. With Si/Al ratio improvement, the quantity of strong acid sites showed an obviously decline. From Table II, HS-12.5 possesses the strongest acid quantity of 0.530 mmol/g, and HS-80 possesses the least strong acid quantity of 0.057 mmol/g. It indicates that varying Si/Al ratio in initial gel can adjust Al content in framework and further control the quantity of the Brønsted acid sites. From Fig. 5, the peak center of strong acid sites shifts to lower temperature with Si/Al ratio improvement. It could correspond to the decrease of the paired Al sites in the framework of SSZ-13.
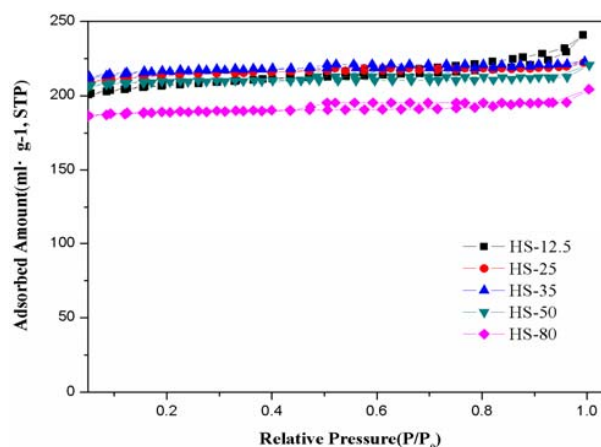

Fig. 4 N_2 adsorption/desorption of SSZ-13 samples

TABLE II
ACID PROPERTIES FOR SSZ-13

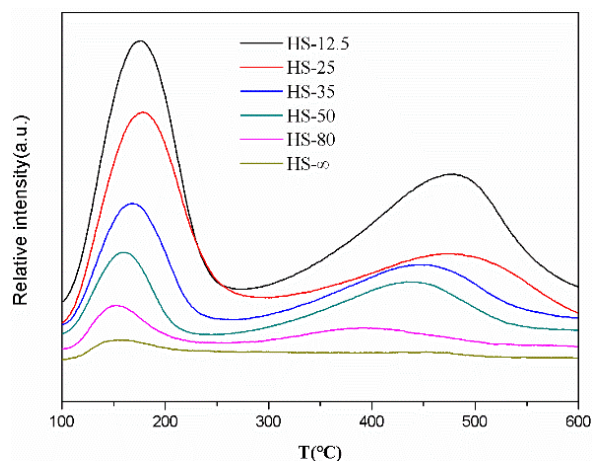| Sample	Weak acid center (°C)	Strong acid center (°C)	Acid site density by NH_3 (mmol/g)
HS-12.5	175.5	479.1	0.530
HS-25	170.1	463.1	0.412
HS-35	167.2	452.6	0.300
HS-50	160.8	433.5	0.260
HS-80	151.0	389.8	0.057

Fig. 5 NH_3-TPD of the of all samples

Figs. 6 and 7 show the methanol conversion and selectivities to ethylene and propylene of SSZ-13 samples respectively. During the initial stage of MTO reaction, the methanol conversion of all samples can be kept at 100%. The

methanol conversion will decline as MTO reaction progresses. The SSZ-13 samples with different Si/Al ratio show different catalyst lifetime. HS-35 shows the longest lifetime. Zhu et al. [17] and Dahl et al. [4] found that the increase of Si/Al ratio could improve the lifetime of SSZ-13, which seems to be inconsistent with our results of catalytic performance test. According to the preceding results of SEM, the amount of Al source has an impact on the morphology of SSZ-13 particles. With lower Si/Al ratio, the particle size of SSZ-13 can decrease evidently. Small crystal size can accelerate methanol and product diffusion rate. More cages in SSZ-13 particles can be active by coke species inside. Although HS-50 and HS-80 show lower acid amounts and strength according to NH_3-TP, there are abundant cages which could not be active due to their micron-sized crystal particles, leading to the rapid deactivation. It proves that catalyst particles size has a great impact on the MTO catalytic properties. When the size of samples grains is approximate, SSZ-13 with higher Si/Al ratio shows a longer lifetime. Hence, HS-35 shows longest lifetime, and the lifetime of HS-80 is longer than that of HS-50.

The selectivities to ethylene and propylene increasing with time on stream could exceed 80% before deactivation. Samples with lower Si/Al ratios exhibit lower initial selectivities to the light olefins. The selectivities to light olefins of HS-80 is 72%, and it is 33% higher than that of HS-12.5. HS-12.5 shows inferior selectivities to ethylene and propylene compared with HS-80 due to higher initial selectivities to light alkanes, mainly propane. The SSZ-13 with lower Si/Al ratios possesses stronger acidity including larger amount of the Brønsted acid sites and more paired Al sites in the framework. Paired Al sites are crucial to the initial propane formation, and samples with lower Si/Al ratios exhibit higher initial selectivities to these light alkane products. Both of these phenomena in the transient behavior of SSZ-13 suggest that the MTO reaction in CHA is being affected by the acid site concentration, thus producing the differing selectivities to alkanes and light olefins observed.
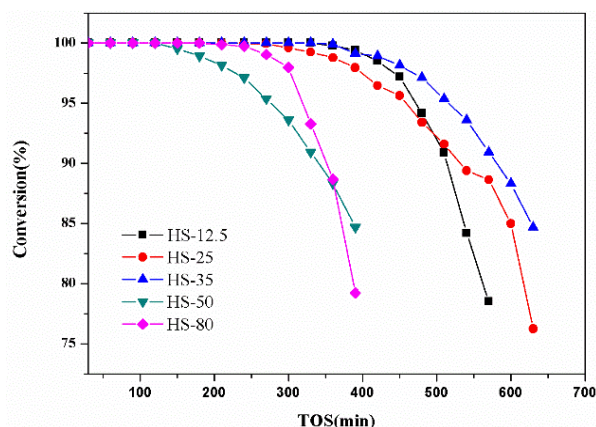
affect zeolites nucleation process at the beginning of hydrothermal reaction. SSZ-13 samples with lower Si/Al ratio possess stronger acidity including larger amount acid sites and stronger acid strength. HS-35 among all the samples possesses the longest lifetime and excellent light olefins selectivity. HS-80 shows the highest initial light olefins selectivity and the rapid deactivation caused by its micro-sized crystal size. In conclusion, the MTO catalytic properties of SSZ-13 were mainly determined by the diffusion distance and acidity.
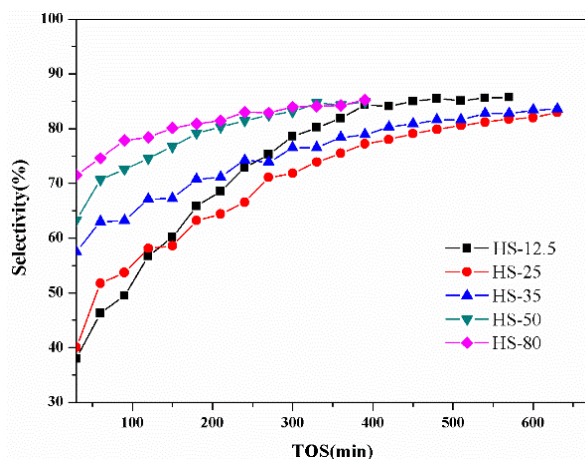

Fig. 7 Selectivities to ethylene and propylene

Common way that improves Si/Al ratio of gel compositions could impair zeolites acidity and enhance the selectivities to light olefins. However, Al source is the key to downsize the crystal size in some specific zeolite synthesis conditions. The decrease of Si/Al ratio could enlarge crystal size and lengthen diffusion way make underutilization of cages. The way to synthesize nano-sized or mesoporous SSZ-13 with high Si/Al ratios is expected to be explored further.

REFERENCES

[1] P. Tian, Y. Wei, M. Ye, Z. Liu. "Methanol to Olefins (MTO): From Fundamentals to Commercialization," in *ACS Catalysis*. vol 5, 2015, pp 1922-38.
[2] M. Stöcker. "Methanol-to-hydrocarbons: catalytic materials and their behavior1," in *Microporous and Mesoporous Materials*. vol 29, 1999, pp 3-48.
[3] L. Wu, E. J. M. Hensen. "Comparison of mesoporous SSZ-13 and SAPO-34 zeolite catalysts for the methanol-to-olefins reaction," in *Catalysis Today*. vol 235, 2014, pp 160-8.
[4] L. Wu, V. Degirmenci, P. C. M. M. Magusin, N. J. H. G. M. Lousberg, E. J. M. Hensen. "Mesoporous SSZ-13 zeolite prepared by a dual-template method with improved performance in the methanol-to-olefins reaction," in *Journal of Catalysis*. vol 298, 2013, pp 27-40.
[5] E. Borodina, F. Meirer, I. Lezcano-González, M. Mokhtar, A. M. Asiri, S. A. Al-Thabaiti, B. M. Weckhuysen. "Influence of the Reaction Temperature on the Nature of the Active and Deactivating Species during Methanol to Olefins Conversion over H-SSZ-13," in *ACS Catalysis*. vol 5, 2015, pp 992-1003.

Fig. 6 Catalytic conversion of methanol

IV. CONCLUSION

The amount of Al composition in SSZ-13 precursor can

[6]   M. A. Deimund, L. Harrison, J. D. Lunn, Y. Liu, A. Malek, R. Shayib, M. E. Davis. "Effect of Heteroatom Concentration in SSZ-13 on the Methanol-to-Olefins Reaction," in *ACS Catalysis*. vol 6, 2016, pp 542-50.

[7]   C. Gonzalez-Arellano, A. Grau-Atienza, E. Serrano, A. A. Romero, J. Garcia-Martinez, R. Luque. "The role of mesoporosity and Si/Al ratio in the catalytic etherification of glycerol with benzyl alcohol using ZSM-5 zeolites," in *Journal of Molecular Catalysis* A: Chemical. vol 406, 2015, pp 40-5.

[8]   K. Sato, Y. Nishimura, N. Matsubayashi, M. Imamura, H. Shimada. "Structural changes of Y zeolites during ion exchange treatment: effects of Si/Al ratio of the starting NaY," in *Microporous and Mesoporous Materials*. vol 59, 2003, pp 133-46.

[9]   L. Shirazi, E. Jamshidi, M. R. Ghasemi. "The effect of Si/Al ratio of ZSM-5 zeolite on its morphology, acidity and crystal size,"in Crystal Research and Technology. vol 43, 2008, pp 1300-6.

[10] A. Simon-Masseron, J. P. Marques, J. M. Lopes, F. R. Ribeiro, I. Gener, M. Guisnet. "Influence of the Si/Al ratio and crystal size on the acidity and activity of HBEA zeolites," in *Applied Catalysis A: General*. vol 316, 2007, pp 75-82.

[11] N. Nishiyama, M. Kawaguchi, Y. Hirota, D. Van Vu, Y. Egashira, K. Ueyama. "Size control of SAPO-34 crystals and their catalyst lifetime in the methanol-to-olefin reaction," in *Applied Catalysis A: General*. vol 362, 2009, pp 193-9.

[12] S. R. Venna, M. A. Carreon. "Synthesis of SAPO-34 Crystals in the Presence of Crystal Growth Inhibitors," in *The Journal of Physical Chemistry B*. vol 112, 2008, pp 16261-5.

[13] P. Wang, D. Yang, J. Hu, J. a. Xu, G. Lu. "Synthesis of SAPO-34 with small and tunable crystallite size by two-step hydrothermal crystallization and its catalytic performance for MTO reaction," in *Catalysis Today*. vol 212, 2013, pp 62.e1-.e8.

[14] Z. Li, M. T. Navarro, J. Martínez-Triguero, J. Yu, A. Corma. "Synthesis of nano-SSZ-13 and its application in the reaction of methanol to olefins," in *Catalysis Science & Technology*. vol 6, 2016, pp 5856-63.

[15] M. Kumar, H. Luo, Y. Roman-Leshkov, J. D. Rimer. "SSZ-13 Crystallization by Particle Attachment and Deterministic Pathways to Crystal Size Control," in *Journal of the American Chemical Society*. vol 137, 2015, pp 13007-17.

[16] S. Bordiga, L. Regli, D. Cocina, C. Lamberti, M. Bjørgen, K. P. Lillerud. "Assessing the Acidity of High Silica Chabazite H−SSZ-13 by FTIR Using CO as Molecular Probe: Comparison with H−SAPO-34," in *The Journal of Physical Chemistry B*. vol 109, 2005, pp 2779-84.

[17] Q. Zhu, J. N. Kondo, R. Ohnuma, Y. Kubota, M. Yamaguchi, T. Tatsumi. "The study of methanol-to-olefin over proton type aluminosilicate CHA zeolites," in *Microporous and Mesoporous Materials*. vol 112, 2008, pp 153-61.